Epitaxial growth on gas cluster ion-beam processed GaSb substrates using molecular-beam epitaxy

K. Krishnaswami, S. R. Vangala, B. Zhu, and W. D. Goodhue[a)]
Photonics Center, Department of Physics and Applied Physics, University of Massachusetts, Lowell, Massachusetts 01854

L. P. Allen[b)] and C. Santeufemio
Epion Corporation, Billerica, Massachusetts 01821

X. Liu, M. C. Ospina, J. Whitten, and C. Sung
Center for Advanced Material, University of Massachusetts, Lowell, Massachusetts 01854

H. Dauplaise and D. Bliss
Air Force Research Laboratory/SNHC, Hanscom Air Force Base, Massachusetts 01731

G. Dallas and D. Bakken
Galaxy Compound Semiconductors, Spokane, Washington 99206

K. S. Jones
Department of Materials Science, University of Florida, Gainesville, Florida 32611

(Received 27 October 2003; accepted 1 March 2004; published 8 June 2004)

Chemical mechanical polished (CMP) (100) GaSb substrates were processed using gas cluster ion beams (GCIB) to improve surface smoothness, reduce subsurface damage, and produce a thermally desorbable oxide layer for molecular-beam epitaxy (MBE) overgrowth. In this article, we report the growth of GaSb/AlGaSb epilayers on GCIB processed GaSb substrates. The substrates were processed using either O_2 or CF_4/O_2 as the gas cluster in a dual-energy recipe that included a moderate energy (10 keV) etch step followed by a low-energy (3 keV) smoothing step, with a relatively low total dose of 4×10^{15} ions/cm^2. Half of each wafer was masked such that the epitaxial layers were grown on both CMP and GCIB polished surfaces. Atomic force microscopy showed the elimination of CMP surface scratches on the GCIB processed surfaces. X-ray photoelectron spectroscopy results indicate that the surface oxide composition and thickness can be engineered through the GCIB process recipes. AlGaSb marker layers were used to chart the evolution of the overgrown layers. Cross-sectional transmission electron microscope images of the substrate/epi-interface show that the CMP finished regions contained defects that propagated into the epilayers as compared to the GCIB finished region that showed no penetrating defects, indicating an improved substrate/epi-interface. This work demonstrated that GCIB processing of semiconductor materials has the potential to produce ''epiready'' surfaces. © *2004 American Vacuum Society.*
[DOI: 10.1116/1.1714917]

I. INTRODUCTION

The growth in power-consumption levels as integrated circuits increase in size and functionality, coupled with the ever increasing demand for portable electronics, has provided the semiconductor industry with the impetus to investigate a class of materials and devices for applications in the area of low-power electronics. Circuit architectures, predicated on antimonide-based III–V materials, are currently under investigation as they operate at low supply voltages without sacrificing performance.

Antimonide-based compound semiconductors (ABCS) are also promising candidates as ''barrier materials'' for optoelectronic and wireless devices that operate in the terahertz or mid-infrared region from 8–14 μm.[1] ABCS material properties, such as low effective electron/hole mass, high mobility, and low threshold voltage operation,[2] have led to high-quantum-efficiency photodetectors,[3] thermophotovoltaic devices,[4] avalanche photodiodes,[5] tunnel switch diodes,[6] high-reflectivity Bragg reflectors for 1.5 μm communications,[7] and room-temperature mid-infrared region quantum-well laser diodes.[8] In order to fabricate such optoelectronic devices, it is necessary to have a substrate that can support epitaxial growth of ternary and quaternary materials that cover a wide spectral range, from 0.3 to 1.58 eV, or from the band gap of InAs to the band gap of AlSb. Among the ABCS family, the GaSb substrate is particularly well suited for this task owing to its lattice parameter of 0.609 nm, which is between those of InAs and AlSb (0.606 and 0.614 nm, respectively). The difficulty in producing defect- and damage-free GaSb substrate surfaces with a thin thermally desorbable surface oxide presently inhibits wider-scale commercial applications of the material.

Recent investigations have focused on understanding GaSb oxide formation and the development of etch techniques to replace the surface oxide produced by chemical

a)Electronic mail: william_goodhue@uml.edu
b)Currently at: Galaxy Semiconductors, Spokane, WA 99206.

mechanical polish (CMP) with a thinner, more stable, and thermally desorbable oxide prior to epitaxial growth. Various methods of oxide preparation have been suggested including wet chemistry,[9–11] ultraviolet radiation,[12] and dry ion etch techniques.[13] However, information regarding surface morphology, evolution of surface species (such as oxides), and variations in surface chemical compositions have not been forthcoming. Most of these processes have their limitations, as they are mostly characterized by high oxidation rates and low solubility of their complex oxide compositions. Although processing substrates with such methods prior to growth has been conducted in the past, development of a final polish and surface preparation technique for GaSb substrates that make them ''epiready'' right out of their shipping container would reduce manufacturing costs and improve yields, thereby making GaSb more commercially attractive.

Recently, gas cluster ion beam (GCIB) processing[14] has been shown to be a promising technique in smoothing GaSb substrates[15] with several recipes demonstrating the smoothing of CMP-processed GaSb surfaces. Each recipe produces a characteristic oxide layer, the stoichiometry of which depends on the reactive gas employed.[16] In this article, we demonstrate the ability to thermally desorb the oxide layer and grow epitaxial layers directly on GCIB smoothed GaSb surfaces. The GCIB surface oxides are evaluated with x-ray photoelectron spectroscopy (XPS), spectroscopic ellipsometry (SE), refection high-energy electron diffraction (RHEED) analysis, and atomic force microscopy (AFM). The resulting epitaxial layers are evaluated with cross-sectional transmission electron microscopy (XTEM), and secondary ion mass spectrometry (SIMS).

II. EXPERIMENT

GaSb substrates were cut to within $\pm 0.5°$ of the (100) crystal orientation and CMP processed to provide a smooth surface. Due to its soft nature, standard CMP techniques result in an average roughness of $R_a \sim 3$ to 10 Å, often accompanied with shallow surface scratches and associated subsurface damage. Based on our previous work,[15,16] two dual-energy single gas GCIB processes were selected to improve the finish of CMP-processed substrates normally supplied for epitaxial growth. An Ultra-Smoother II GCIB instrument (Epion Corp., Billerica, MA), used for smoothing a wide variety of material surfaces, was implemented for the GaSb surface process. The selected recipes were:

(1) GCIB process A (O_2-GCIB)-10 keV O_2 etch step followed by a 3 keV O_2 smoothing step with a total charge fluence of 4×10^{15} ions/cm^2, and
(2) GCIB process B (CF_4/O_2-GCIB)-10 keV CF_4/O_2 etch step followed by a 3 keV CF_4/O_2 smoothing step with a total charge fluence of 4×10^{15} ions/cm^2.

In order to effectively compare the GCIB polishing technique to the CMP-processed technique as a substrate preparation method for MBE growth, half of the GaSb wafer was masked during GCIB processing to provide both CMP- and GCIB-processed regions on the same substrate. Thus, simultaneous MBE growth on both regions with identical system parameters was possible. As a reference, a stand-alone CMP finished surface was also used for overgrowth.

TABLE I. AFM measurements on a representative 10×10 μm sample area of pre- and post-GCIB surfaces.

	O_2-based GCIB		CF_4/O_2-based GCIB	
	Pre-GCIB (CMP)	Post-GCIB	Pre-GCIB (CMP)	Post-GCIB
R_a (nm)	0.25	0.38	0.29	0.19
Z (nm)	5.6	15.7	7.4	3.3
rms (nm)	0.32	0.5	0.35	0.23

GaSb substrates were indium bonded at ~200 °C in air and introduced into the load/outgas chamber of the MBE system (Riber R&D2300) where they were heated to 300 °C and outgassed at 5×10^{-8} Torr. Comparisons of SE measurements of the GaSb surfaces before and after heating showed no change in the thickness, index, and extinction coefficients of the oxide surfaces. The indium bonded substrates were transferred into the growth chamber and heated to 500 °C. Sb flux was introduced once the substrate temperature reached 400 °C to provide an Sb-rich environment during oxide desorption and epigrowth. Flux measurements prior to epigrowth indicated beam-equivalent pressures of $\sim2.9\times10^{-7}$ Torr for Ga, $\sim3.3\times10^{-6}$ Torr for Sb, and $\sim8\times10^{-8}$ Torr for Al.

The oxide layers were desorbed at 550 °C, 560 °C, and 530 °C (substrate block thermocouple reading) for the respective CMP, O_2-GCIB, and CF_4/O_2-GCIB surfaces. The desorption was monitored by observing the development of near-streak patterns on the RHEED screen. However, the substrate temperature was briefly raised to 560 °C for all surfaces in an attempt to ensure complete desorption. Standard wet-etched GaSb samples showed oxide desorption at 530 °C with strong RHEED patterns. Upon desorption, the substrate temperature was reduced to a growth temperature of 500 °C. Starting with a homoepitaxial layer of GaSb, six periods of GaSb/AlGaSb layers were grown on the GCIB-finished substrates while only a homoepitaxial layer was on the CMP-finished substrate. The AlGaSb layers on the GCIB-finished substrates were used as marker layers to determine the evolution of the growing surface. All growth runs lasted for about 1 h with a growth rate of ~1 μm/h.

III. RESULTS

AFM measurements were made on the GaSb substrates before and after GCIB processing to evaluate the surface roughness of a sample area of 10×10 μm^2, a sample area relevant to device metrology. AFM results are provided in Table I, where R_a is a measure of the mean roughness, rms is the root mean square roughness, and Z is the peak-to-valley height difference. Compared to CMP surfaces, the O_2-GCIB process increased R_a by ~0.13 nm and Z by ~10 nm while the CF_4/O_2-GCIB process reduced R_a by 0.1 nm and Z by

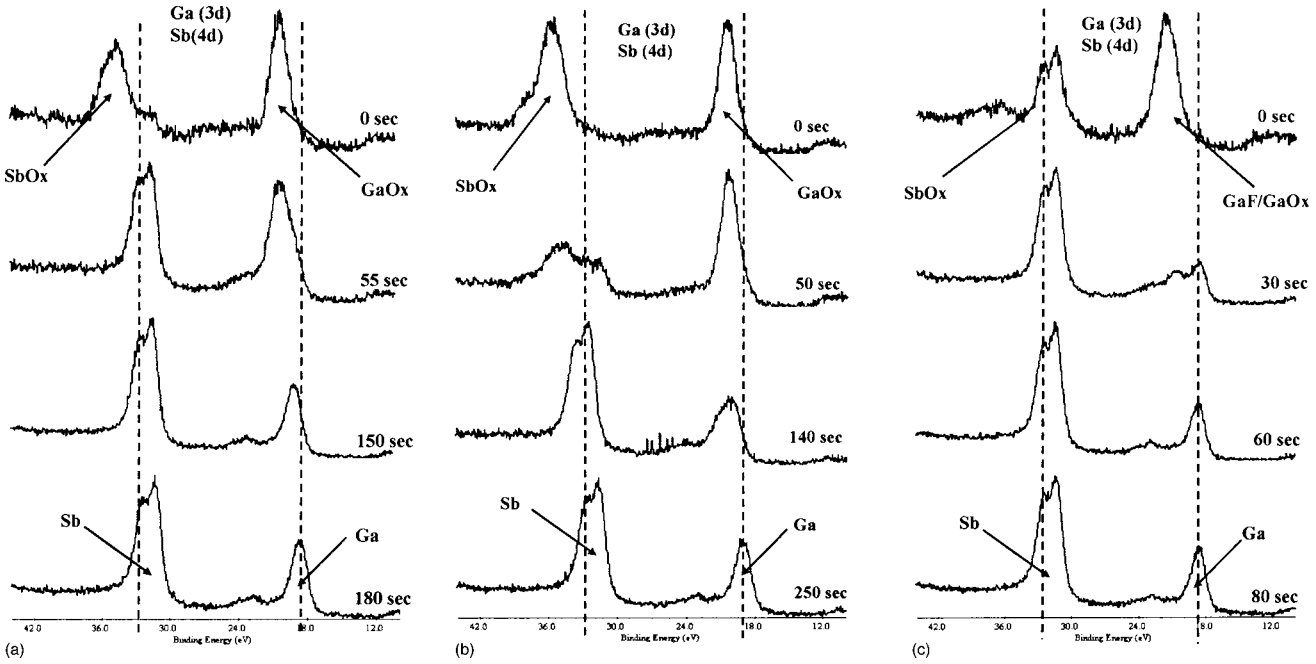

FIG. 1. XPS spectra and depth profile as a function of sputtering time for: (a) CMP-, (b) O_2-GCIB-, and (c) CF_4/O_2-GCIB-finished GaSb substrates.

4.1 nm. From these measurements, the CF_4/O_2-GCIB process produced a GaSb surface with lower surface roughness as compared to the O_2-GCIB process.

XPS spectra were obtained using a VG ESCALAB instrument (Thermo Vacuum Generators, Hastings, UK) equipped with a Mg $K\alpha$ X-ray source and a concentric hemispherical analyzer detector. *In situ* sputtering for depth profiling was carried out with a 5 keV argon-ion gun with a typical ion beam current of $\sim$100 μA covering approximately the entire portion of the 1 cm^2 sample. Figures 1(a)–1(c) shows XPS spectra of the CMP-, O_2-GCIB-, and CF_4/O_2-GCIB-finished samples, respectively, as a function of sputter time, which was then correlated to depth using a SE. The surface oxide composition of the CMP-finished surface contains both Ga and Sb oxides, as shown in Fig. 1(a), with mostly Sb oxides in the near-surface region and mostly Ga oxides near the substrate interface. The thickness of this oxide was measured to be 11.3 nm, requiring a sputter time of $\sim$180 s to remove it from the substrate surface. In the case of the O_2-GCIB sample, shown in Fig. 1(b), Ga and Sb oxides are distributed fairly uniformly throughout its 28.6 nm thickness, requiring 250 s of sputtering for removal. The spectra for CF_4/O_2-GCIB, shown in Fig. 1(c), indicate Ga and Sb oxides at the surface prior to sputtering. The higher binding energy for the Ga 3*d* peak and its greater width compared to the other two samples is likely due to GaF_x formation. This is consistent with the presence of fluorine on the surface, as indicated by F 1*s* detection observed in the survey scan. In this case, sputtering readily reduces the intensity of the fluorine-induced Ga peak, indicating that fluorides reside mainly on the surface of the oxide layer. This oxide layer, measured to be 6.4 nm thick, requires only 80 s of sputtering to completely remove from the substrate surface.

SE measurements results of the optical parameters for pre- and postheated CMP, O_2-GCIB, and CF_4/O_2-GCIB surfaces (performed during wafer mounting) were within statistical variations of each other. This indicated that indium bonding of the GaSb substrates at $\sim$185 °C in air did not change the characteristics of the oxide layer.

XTEM images of GaSb homoepitaxy on the CMP- and GCIB-processed substrates were obtained to evaluate both the substrate/epi-interface, as well as the evolution of the growing surface, by examining the AlGaSb/GaSb heterostructures. XTEM images of representative areas were acquired for the sample that contained epigrowth on both CMP and O_2-GCIB surfaces, shown in Fig. 2. A dark-field image with a [200] two-beam condition reflection was employed in Fig. 2 in order to image the contrast between the GaSb and AlGaSb layers. The two images show a dislocation layer $\sim$600 Å wide at the substrate/epi-interface followed by $\sim$550 Å of GaSb homoepitaxy. The growth structure continues with six periods of AlGaSb and GaSb, each $\sim$120 Å and $\sim$1400 Å respectively, with a final cap layer of GaSb.

Figure 2(a) shows a low magnification image of the epilayers on the CMP-finished substrate that clearly shows the presence of a pit which is $\sim$80 Å in height. This feature would not have been noticed if the epilayer was not marked, since it corrected itself within $\sim$100 nm of growth and did not propagate to the second marker layer. In contrast, the low magnification image of the O_2-GCIB-finished surface, shown in Fig. 2(b), showed that the interface defects did not propagate into the growing epilayers. Epitaxial growth on both CMP-finished surfaces showed extremely rough substrate/epi-interfaces with the presence of stacking faults and microvoids that originate at the interface, shown in Figs. 3(a) and 3(b). Figures 3(c) and 3(d) show high-resolution

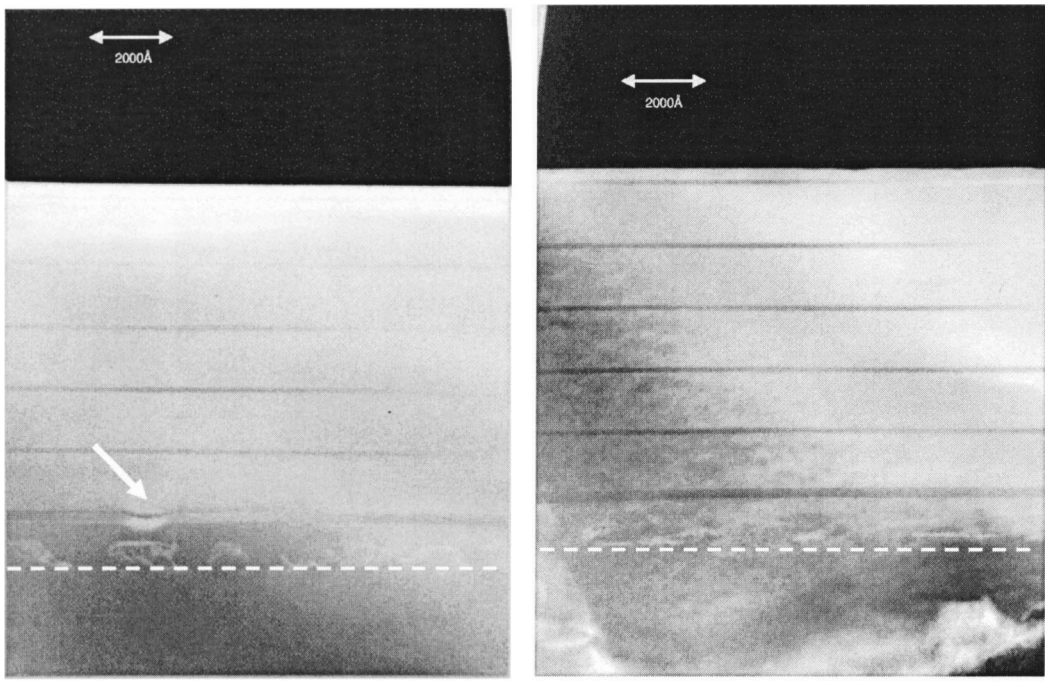

FIG. 2. XTEM images of epi-growth GaSb/AlGaSb on: (a) CMP- and (b) O_2-GCIB-finished surfaces. It clearly shows pitting in the CMP finished epilayer as compared to the GCIB finished surface where the interface defects do not propagate into the growing layers. However, this defect does not propagate beyond the second marker layer. The dotted lines indicate the substrate/epi-interface.

XTEM images of overgrown epilayers on the O_2-GCIB- and CF_4/O_2-GCIB-processed GaSb substrates, respectively. Both images show the presence of a dislocation layer and a smooth transition to the first marker layer with no interface defect penetration.

SIMS profile measurements were made at the substrate/epi-interface and on the epilayers grown on the CMP- and O_2-GCIB-finished samples. These measurements are probable upper limits for the analyzed species since there may be unresolved mass interferences. The areal density of carbon detected at the interface of the CMP surface was $\sim 7.8 \times 10^{14}$ atoms/cm^2, more than twice the amount detected for O_2-GCIB surfaces. The O_2-GCIB samples showed an areal density of $\sim 5.7 \times 10^{14}$ atoms/cm^2 for oxygen, an order of magnitude higher than that of the CMP surfaces. Both CMP and O_2-GCIB surfaces showed the presence of beryllium at the interface with areal densities of $\sim 1.1 \times 10^{15}$ and $\sim 8.4 \times 10^{13}$ atoms/cm^2, respectively. The presence of indium was detected in all the epitaxial layers indicating contamination from indium bonding substrates to the molybdenum blocks. SIMS results also indicated a higher level of other impurities (S, Si, Fe, Ni, and W) in the O_2-GCIB-processed surfaces as compared to the CMP surfaces.

IV. DISCUSSION

Although RHEED pattern analysis, just prior to overgrowth, indicates the desorption of the oxide layers, the GCIB-processed samples showed patterns that were weaker and spottier as compared to wet-etched CMP samples. We suspect that the oxide layers on these samples had not fully desorbed. This problem was even more severe when using CMP-processed surfaces. Incomplete desorption leaves nanoscale and angstrom-scale oxide islands which are bridged during overgrowth. Voids are generated over the larger islands and faults are generated over the smaller is-

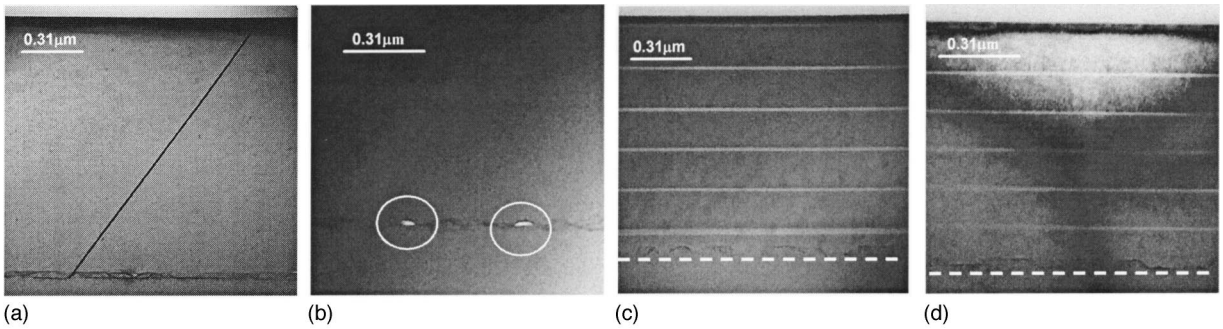

FIG. 3. XTEM images of MBE overgrowth on CMP- and GCIB-finished GaSb wafers. Overgrowth on the CMP-finished surface showed the presence of: (a) Stacking faults and (b) microvoids that originated at the interface. Overgrowth on: (c) O_2-GCIB and (d) CF_4/O_2-GCIB showed a smooth transition from the dislocation layer to the epilayers. The dotted lines indicate the substrate/epi-interface.

lands that generally remain confined to the interface area. However, with the recipes employed to date, the GCIB processes have not been able to produce a fully desorbable oxide layer and thus, continue to show the presence of a dislocation layer at the substrate/epi-interface. A change in GCIB recipe will be required to fully eliminate this problem.

Of the two selected processes, CF_4/O_2-GCIB appeared to be better as it produced the smoothest surface and also the thinnest oxide layer. However, this process left a fluorine polymer on the oxide surface which took a substantially longer time (by about a factor of 4) to outgas, as compared to the O_2-GCIB surface. XPS measurements with a thermal stage confirmed the presence of fluorine on the oxide surface, requiring a substrate temperature of $\sim 400\,^{\circ}\mathrm{C}$ to completely liberate. Recently, a low-energy O_2 process as the smoothing step, instead of the second low-energy CF_4/O_2 step, has been implemented as a compromise to reduce outgas time while still retaining a good final polish.

The SIMS results indicated an encouraging decrease in the interfacial carbon in the O_2-GCIB sample over the CMP sample. The higher areal density of oxygen in the O_2-GCIB sample may mean that some atomic mixing (e.g., ion implantation) and reactivity occurred during GCIB processing. The metals that appeared at the interface of the O_2-GCIB-processed surfaces are probably due to contamination from the filament, stainless-steel parts, and residue from prior unrelated samples processed in this GCIB system. The high S and Si content at the interface of the O_2-GCIB-processed sample is also probably due to contamination from previous samples and GCIB recipes. Such cross-contamination issues, however, can be easily resolved by using a dedicated instrument. The source for the high level of beryllium detected at the interface of both CMP and GCIB samples is uncertain at this time.

The AlGaSb marker layers have been very useful in determining the growth geometry of the evolving surface. As confirmed by numerous XTEM images of the GaSb substrate to epi-interface, both the kinetics and thermodynamics of the epigrowth promote a (100) planarization of the layers as the growth progresses. This tendency can be further exploited through the acceptance of a slightly rougher GaSb surface ($R_a > 2$ Å) for overgrowth, especially if the oxide has been established as one that is able to desorb in an MBE growth chamber. Our current work with bromine dry etching may provide a viable course for surface preparation of GaSb substrates. Rather than a fluorine process, the addition of bromine in the GCIB source or its introduction as a background pressure in the target chamber may produce the required high-quality desorbable oxide.

V. CONCLUSION

This research has shown that the GCIB process improves surface roughness and simultaneously produces a desorbable oxide layer, characteristics necessary for defect-free epitaxial growth. In addition, oxide desorbtion and epitaxial overgrowth using MBE on GCIB-finished GaSb substrates have been demonstrated. Results of the epitaxial growth show significantly reduced interface dislocations and a lack of pitting for epitaxy on the GCIB surfaces as compared to the as-received CMP surfaces. By adjusting the GCIB process, residual defects at the substrate/epi-interface can be further reduced.

ACKNOWLEDGMENTS

The authors wish to thank Tom Tetreault of Epion Corporation for helpful suggestions regarding the XPS spectra of the CMP and GCIB samples. The support of DARPA under the ABCS Contract No. F49620-01-1-0514 and the United States Army under Contract No. DAAH01-03-CR018 is gratefully acknowledged. The opinions, interpretations, conclusions, and recommendations are those of the authors and not necessarily endorsed by the United States Air Force and Army.

[1]H. Xie, J. Piao, J. Katz, and W. I. Wang, J. Appl. Phys. **70**, 3152 (1991).
[2]P. S. Dutta, H. L. Bhatt, and V. Kumar, J. Appl. Phys. **81**, 5821 (1997).
[3]O. Hildebrand, W. Kuebart, K. W. Benz, and M. H. Pilkuhn, Appl. Phys. Lett. **37**, 801 (1980).
[4]L. M. Frass, G. R. Girard, J. E. Avery, B. A. Arau, V. S. Sundaram, A. G. Thompson, and J. M. Gee, J. Appl. Phys. **66**, 3866 (1989).
[5]X-C. Cheng and T. C. Mcgill, J. Appl. Phys. **86**, 4576 (1999).
[6]X.-C. Cheng, X. Cartoixa, M. A. Barton, C. J. Hill, and T. C. McGill, J. Appl. Phys. **88**, 6948 (2000).
[7]B. Lambert, Y. Toudic, M. Baudet, B. Guenais, B. Deveaud, I. Valiente, and J. C. Simon, Appl. Phys. Lett. **64**, 690 (1994).
[8]C. Mermelstein, S. Simanowski, M. Mayer, R. Kiefer, J. Schmitz, M. Walther, and J. Wagner, Appl. Phys. Lett. **77**, 1581 (2000).
[9]Z. Y. Liu, B. Hawkins, and T. F. Keuch, J. Vac. Sci. Technol. B **21**, 71 (2003).
[10]E. Papis, A. Piotrowska, E. Kaminska, K. Golaszewska, W. Jung, J. Katcki, A. Kudla, M. Piskorski, T. T. Piotrowski, and J. Adamczewska, Vacuum **57**, 171 (2000).
[11]M. A. Marciniak, R. L. Hengehold, Y. K. Yeo, and G. W. Turner, J. Appl. Phys. **84**, 480 (1998).
[12]N. Bertu, M. Nouaoura, J. Bonnet, L. Lassabatere, E. Bedel, and M. Mamy, J. Vac. Sci. Technol. A **15**, 2043 (1997).
[13]G. Nagy, R. U. Ahmad, M. Levy, R. M. Osgood, M. J. Manfra, and G. W. Turner, Appl. Phys. Lett. **72**, 1350 (1998).
[14]I. Yamada, J. Matsuo, N. Toyoda, and A. Kirkpatrick, Mater. Sci. Eng., R. **34**, 231 (2001).
[15]X. Li, W. D. Goodhue, C. Santeufemio, R. MacCrimmon, L. P. Allen, K. Krishnaswami, D. Bliss, and C. Sung, Appl. Surf. Sci. **218**, 251 (2003).
[16]L. P. Allen, T. G. Tetrault, C. Santeufemio, M. Tabat, X. Li, W. Goodhue, D. Bliss, K. S. Jones, G. Dallas, D. Bakken, and C. Sung, J. Electron. Mater. **32**, 842 (2003).